

# Effect of moving surface on the aerodynamic drag of road vehicles

S N Singh<sup>1\*</sup>, L Rai<sup>2</sup>, P Puri<sup>2</sup>, and A Bhatnagar<sup>1</sup>

<sup>1</sup>Department of Applied Mechanics, Indian Institute of Technology, Delhi, India

<sup>2</sup>Department of Mechanical Engineering, Indian Institute of Technology, Delhi, India

*The manuscript was received on 20 March 2004 and was accepted after revision for publication on 11 August 2004.*

DOI: 10.1243/095440705X5886

**Abstract:** The effect on aerodynamic drag using a model of a truck has been investigated by controlling the boundary layer separation by the momentum injection method using a rotating cylinder. It involves the use of experiments coupled with computational fluid dynamics (CFD) analysis to validate the theory of momentum injection. Modelling of the truck has been done on the software GAMBIT<sup>®</sup>. The best suitable turbulence model was selected by comparing the results with the experimental results. The rotational speed and radius of the cylinder are varied to establish the effect of momentum injection on aerodynamic drag. The coefficient of drag reduces by approximately 35 per cent from an initial value of 0.51–0.32 for a cylinder of radius 1 cm with rotational speed of 4000 r/min.

**Keywords:** aerodynamic drag, boundary layer control, computational fluid dynamics, moving surface, momentum injection, road vehicles

## 1 INTRODUCTION

Computational fluid dynamics (CFD) is being used intensively in unravelling the complex fluid-flow phenomenon for both internal and external flows. In the present study CFD is used to study the aerodynamic drag on road vehicles, especially trucks. Aerodynamic drag on vehicles can be reduced either by streamlining the body or by controlling the boundary layer separation. One of the methods used to control the boundary layer has been momentum injection, which has been applied in other countries on road vehicles whereby a drag reduction of approximately 2–6 per cent resulted in a significant reduction in fuel consumption. For instance, the prototype FEV 2000 achieves a reduction of drag by as much as 57 per cent and a resultant fuel saving of up to 40 per cent [1]. The effect of drag on the moving vehicle is proportional to the square of velocity, so with increase in velocity (at approximately 50 km/h), aerodynamic drag becomes one of the most prominent factors contributing to the total drag experienced by the vehicle. As the road infrastructure is

improving in India, an increase in speed would result in high aerodynamic drag, which needs to be looked into. All these factors provide a highly motivating area of immense potential, which if exploited and used could be greatly beneficial to the economy of the nation.

From the time Prandtl introduced the boundary layer concept, scientists and engineers have been faced with a constant challenge to reduce the adverse effects of boundary layer separation on the performance of various devices such as airfoils, compressor blades, turbine blades, etc. Boundary layer separation takes place under adverse pressure gradient conditions when viscous effects are no longer confined to a thin layer but affect the overall flow pattern drastically. The most common application to date has been the flow around an aerofoil wing of an aircraft. Flow separation takes place on the upper surface of the aerofoil at a large angle of attack resulting in a drastic fall in lift. Several methods, such as mass injection either by blowing or by suction, coating of the wall, or transition to turbulent flow, etc. have been practiced with varying degrees of success. Significant literature has accumulated over the years and has been reviewed rather effectively by several researchers, including Lachmann [2], Goldstein [3], Chang [4], Schlichting [5], Rosenhead [6], and others.

\*Corresponding author: Department of Applied Mechanics, Indian Institute of Technology, Hauz Khas, New Delhi, 110016, India. email: sidhnathsing@hotmail.com

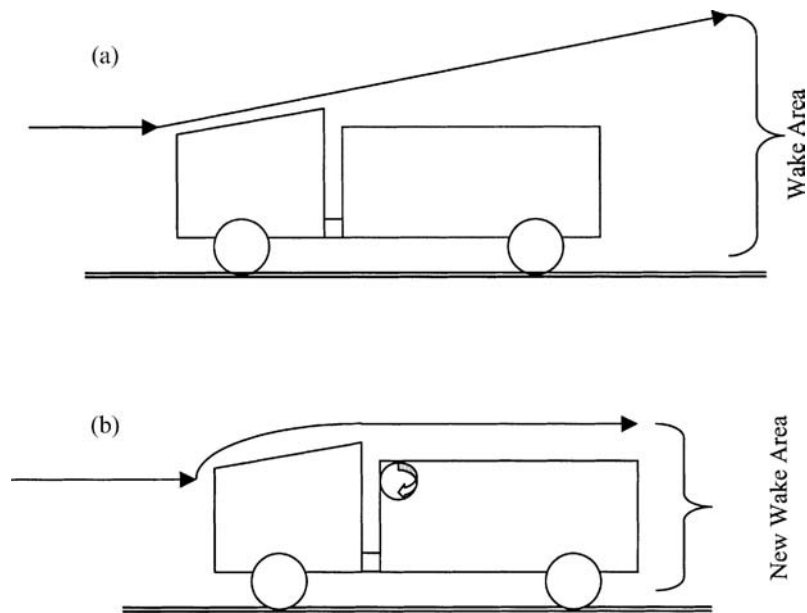


**Fig. 1** Aerodynamic drag: (a) existing situation; (b) expected outcome

The concept of delaying boundary layer separation has also been used in road vehicles to reduce aerodynamic drag. Invariably this has been done by reducing sharp edges to round edges wherever possible. The different techniques used include lip fairing, (Lissaman and Lambie [7]) and guide vanes (Kirsh and Bettes [8] and Montoys and Streers [9]), especially for the roof edges of truck/truck-trailers. Other methods used for altering the flow pattern in tractor-trailers are add-on devices such as roof fairing, sharp edges, or streamlined cabs, which deflect the flow over the trailer in a manner so as to make the tractor-trailer look like a single body (see Chapter 8, reference [1]). However, the use of momentum injection using a moving wall for boundary layer control is still in its nascent stages.

Momentum injection using rotating cylinders has been applied to airfoils in order to improve their lift characteristics [10]. Modi *et al.* [11] applied the concept of moving surface boundary layer control to a Joukowski airfoil using rotating cylinders at the leading and trailing edges of the airfoil. Modi *et al.* [12] assessed the effectiveness of the bound vortex boundary layer control with reference to airfoils modified with a leading edge rotating cylinder. However, the use of rotating cylinders to reduce aerodynamic drag on trucks is a new concept.

A streamlined body shape helps to obtain a low value of drag and the power consumed is significantly affected by the drag force especially at high speeds since,  $\text{power} \propto (\text{velocity})^3$ . Hence, a low drag is highly desirable. To understand this better, con-

sider Fig. 1(a), which shows the flow around an approximate model of an existing truck. The drag force on the truck has two components, namely skin-friction drag and pressure drag (mainly due to separation of boundary layer) [13]. The contribution of pressure drag to the overall drag is very high due to the large size of the wake. The wake area for a rotating cylinder at the end of the front portion (see Fig. 1(b)) is reduced by a large extent as the flow is attached to the body delaying the separation of the boundary layer. This consequentially results in a lower drag and hence lower fuel consumption.

The main aim of the present study is to use a rotating cylinder (in order to inject momentum) to delay the separation of the boundary layer on the top surface of the truck, thereby reducing the aerodynamic drag on the vehicle. This study utilizes both experiments and CFD to analyse the effect of momentum injection on aerodynamic drag. It involves the modelling of the truck on GAMBIT® [14] and solving the flow field around the truck using the CFD software FLUENT® [14] by incorporating different turbulence models available in the software. The theoretical results obtained using these turbulence models are compared with those obtained through experiments to select the best turbulence model.

The use of CFD to solve such problems is a great challenge in itself, as it not only requires proper simulation of conditions and prediction of flows but also a very high degree of accuracy. The accuracy is contingent on the ability to work around the

empirical constraints in the Navier–Stokes equations, which are dependent on different flows. Furthermore, it delves into the effect of various parameters, e.g. boundary conditions, meshing size, etc., on aerodynamic drag. Since most of the work done to date has been predominantly on optimization of design of vehicles such as cars, it is a great challenge to look at other vehicle geometries, such as those of trucks, where there has been significantly less work done. Trucks act as an interesting subject area for the present study because as a result of an increase in speeds due to road improvements, the aerodynamic drag force acting on them is going up considerably.

The present investigation builds on the above body of literature and involves the use of experiments coupled with CFD analysis in order to reduce the aerodynamic drag on trucks using the momentum injection technique of controlling the boundary layer through a rotating cylinder [5].

## 2 MATHEMATICAL FORMULATION

The starting point of any numerical method [15] is the mathematical model, i.e. the set of partial differential or integro-differential equations and boundary conditions. An appropriate model needs to be chosen for the target application (incompressible, inviscid, turbulent, etc.) In FLUENT® a broad range of mathematical models for transport quantities is combined with the ability to model complex geometries. Conservation laws are derived considering a given quantity of matter or control mass and its extensive properties, such as mass, momentum, and energy.

*Mass conservation equation.* The equation of conservation of mass or continuity equation for steady state can be written as

$$\frac{\partial}{\partial x_i}(\rho u_i) = 0 \quad (1)$$

The above equation is the general form of mass conservation equation and is valid for incompressible as well as compressible flows.

*Momentum conservation equation.* Conservation of momentum in the  $i$  direction in an inertial reference frame for steady state is given by

$$\frac{\partial}{\partial x_j}(\rho u_i u_j) = -\frac{\partial p}{\partial x_i} + \frac{\partial \tau_{ij}}{\partial x_j} + \rho g_i + F_i \quad (2)$$

where  $p$  is the static pressure,  $\tau_{ij}$  is the stress tensor, and  $\rho g_i$  and  $F_i$  are the gravitational body force and external body forces respectively. The stress tensor is given by

$$\tau_{ij} = \left[ \mu \left( \frac{\partial u_i}{\partial x_j} + \frac{\partial u_j}{\partial x_i} \right) \right] - \frac{2}{3} \mu \frac{\partial u_k}{\partial x_k} \delta_{ij} \quad (3)$$

Turbulent flows are characterized by fluctuating velocity fields. These fluctuations mix transported quantities, such as momentum, energy, and species concentration, and cause the transported quantities to fluctuate as well. Since these fluctuations can be of small scale and high frequency, they are too computationally expensive to simulate directly in practical engineering calculations. Instead, the instantaneous (exact) governing equations can be time-averaged, ensemble-averaged, or otherwise manipulated to remove the small scales, resulting in a modified set of equations that are computationally less expensive to solve. However, the modified equations contain additional unknown variables and turbulence models are needed to determine these variables in terms of known quantities. Flows and related phenomena can be described by partial differential (or integro-differential) equations, which cannot be solved analytically, except in special cases. To obtain an approximate solution numerically, the discretization method is used, which approximates the differential equations by a system of algebraic equations. The approximations are applied to small domains in space and/or time so the numerical solution provides results at discrete locations in space and time. The accuracy of experimental data depends on the quality of the tools used, whereas the accuracy of numerical solutions is dependent on the quality of the discretization used.

### 2.1 Turbulence model and boundary conditions

The turbulence model used for the final simulation purposes is the Realizable  $k$ - $\varepsilon$  ( $r$ - $k\varepsilon$ ) model, since it best matches with the experimental results. Two-dimensional simulations were performed on the grid generated from GAMBIT®. Two-dimensional simulations are carried out as a first step to understand the flow characteristics due to excessive flow complexities associated with three-dimensional analysis. The flow has been analysed under steady state conditions. The boundary condition for all the boundaries of the truck was set as wall and that for cylinder was kept as moving wall with a specific rotational velocity to be assigned before the start of simulation.

## 2.2 Modelling of the truck and fabrication

The model was tested in a low turbulence, blow-down, open wind tunnel, having the test section as  $0.45 \text{ m} \times 0.75 \text{ m} \times 5.0 \text{ m}$ . The model was mounted in the test section at a distance of  $0.3 \text{ m}$  from the inlet of the test section. A centrifugal blower running at a maximum speed of  $900 \text{ r/min}$  provides the air to the wind tunnel. A three-phase motor of  $22 \text{ kW}$  capacity, having a speed of  $1455 \text{ r/min}$ , drives the blower fan. It is coupled to the fan through a V-belt drive system. The range of air speeds possible in the wind tunnel was from  $5 \text{ m/s}$  to  $35 \text{ m/s}$ .

A section of cross-sectional area of  $20 \text{ cm} \times 20 \text{ cm}$  has been removed from the bottom of the test section to allow for the pressure taps to be connected to the manometers. A pitot static tube has been installed in order to measure the static and dynamic pressures. To measure the velocities in the wake region, a three-hole probe was used instead of the pitot static tube.

A testing model of the truck has been fabricated and is shown in Fig. 2 with all dimensions. The

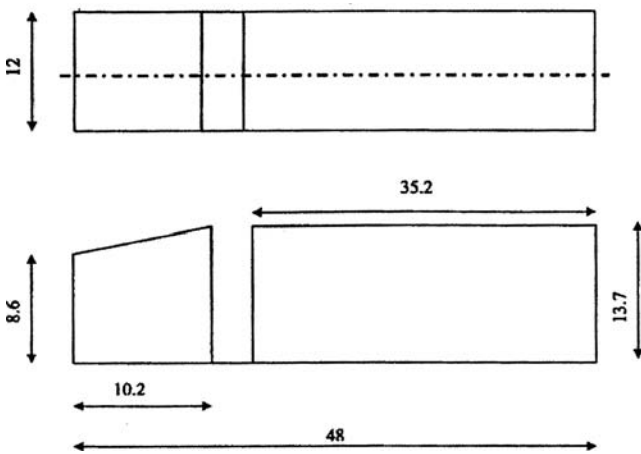


Fig. 2 Top: plan of the testing model; Bottom: elevation of the testing model (all dimensions are in cm)

model was made of wood and was of 1:20 scale. The tyres of the vehicle are not simulated and hence the base of the truck model is placed on the wind tunnel surface. There is no flow beneath the truck. To measure the pressure, 36 pressure taps are provided on the top and rear parts of the model and 12 pressure taps on each side. Thus, in total, 60 pressure taps have been provided on the surface of the model. The taps are made of copper capillary tubes of  $1 \text{ mm}$  diameter each. Two 36-tube manometers were used, inclined at an angle of  $30^\circ$  to the vertical for measurement of pressure from the surfaces of the model with an accuracy of 0.5 per cent. The tests were conducted at a wind tunnel speed of  $26.4 \text{ m/s}$ . The Reynolds number corresponding to this velocity with width as the characteristics length is  $2.04 \times 10^5$ . The free stream velocity in the wind tunnel was measured by a pitot static tube. Figure 3 shows the schematic layout of the tunnel. The maximum frontal area of the model was  $0.01644 \text{ m}^2$  and the blockage created is less than 5 per cent and hence no blockage correction had been done.

## 2.3 Validation of CFD code

For validation of the CFD code FLUENT<sup>®</sup> the results obtained from the experiments are compared with those obtained using FLUENT<sup>®</sup>. This helped in the selection of the best turbulence model and also established the level of accuracy to which the two match. Pressure profiles using four turbulence models, namely Spalart–Allmaras (SA), Standard  $k-\epsilon$  ( $k-\epsilon$ ), Renormalization-group  $k-\epsilon$  (RNG), and Realizable  $k-\epsilon$  ( $r-k\epsilon$ ), were compared with the experimentally obtained pressure distribution on the wall and velocity profile in the wake to select the best suitable turbulence model. Figure 4 shows the comparison of the magnitude of pressure between the four turbulence models and the experimental results. Figure 5 shows the velocity comparison between the

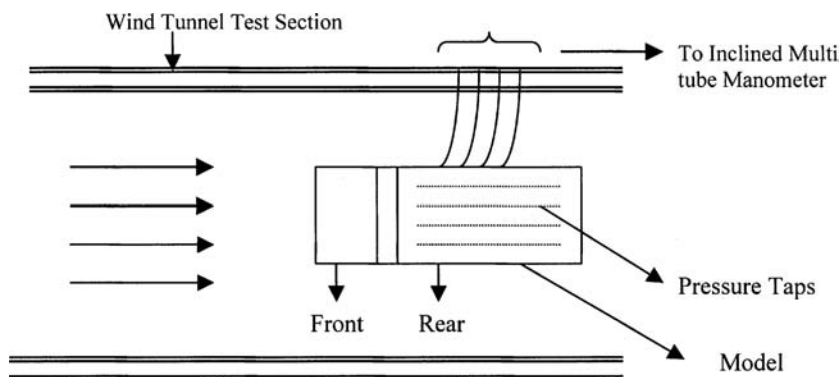


Fig. 3 Schematic layout of the model in the test section of wind tunnel

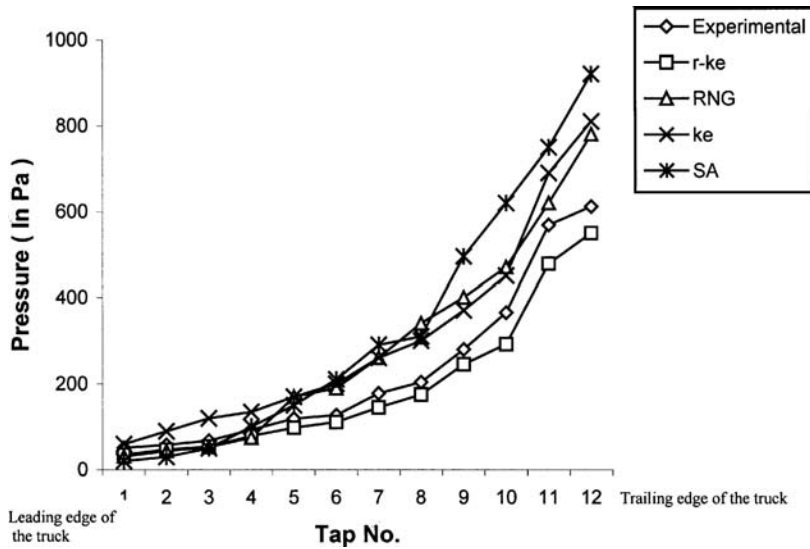


Fig. 4 Comparisons of predicted pressure on the vehicle top surface using different turbulence models

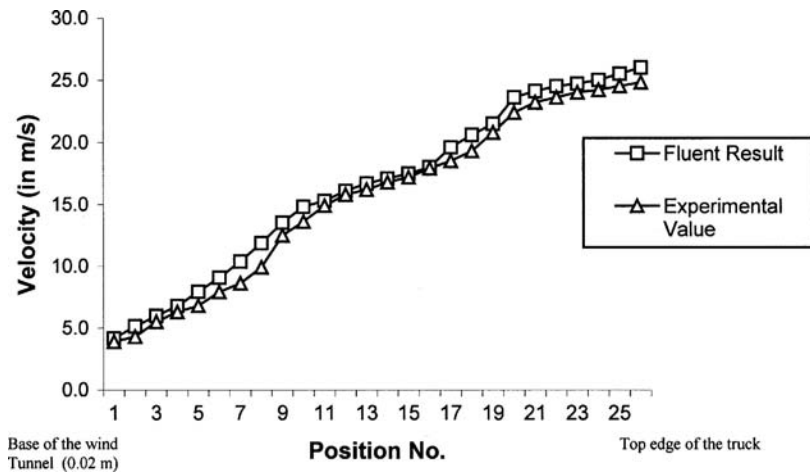


Fig. 5 Velocity profile comparisons in the wake of the vehicle body

experimental and FLUENT® results. The velocities were taken in the downstream of the wake region. From both comparisons it is seen that the Realizable  $k-\epsilon$  turbulence model gives the best match with the experimental results and hence is used for all simulations.

For grid independency, the meshing was refined further until the results were found to be independent of the meshing interval, although other parameters were also checked for grid independency. Table 1 shows in particular the variation of drag coefficient on the model, as the grid was refined. It is seen that for volume cells above 250 000 with cells being closely spaced at the boundaries of the truck, there is no significant variation in the results for drag coefficient.

Table 1 Variation of drag coefficient with finer meshing

No. of cells	Drag coefficient
14 421	0.2
39 348	0.18
51 240	0.39
89 270	0.42
143 641	0.48
267 870	0.51
405 210	0.50

### 3 RESULTS AND DISCUSSION

Having established the validation and grid independency test, further simulations were carried out on a mesh with approximately 420 000 cells with the

adapted-zone method. The simulations are carried out with an air speed of 26.4 m/s with and without the momentum injection technique. The simulations involved two sets of solutions:

- (a) with a cylinder radius of 1 cm;
- (b) with a cylinder radius of 2 cm.

For each set, the rotating speed of the cylinder was varied from 2000 to 6000 r/min ( $\lambda = 0.08\text{--}0.24$ ). Figures 6 and 7 show the wake region in the gap and the rear wall of the truck for no rotation respectively. Figures 8 and 9 depict the suction of flow from the front of the cylinder and injection on the top wall, which was absent in the case of no momentum injection as shown in Figs 6 and 7. There is significant reduction in the wake regions. It is the momentum injection that finally delays the separation and results in reduction of the wake region. The flow without momentum injection resulted in a drag coefficient of 0.51, whereas after the rotation it was seen that the drag coefficient reduced to 0.48.

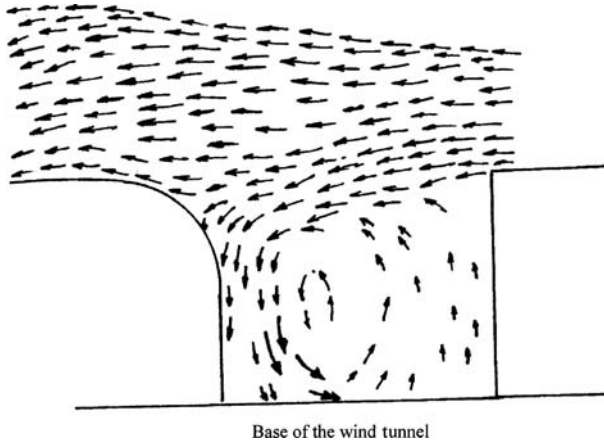


**Fig. 6** Predicted wake region at zero r/min of the cylinder in the gap

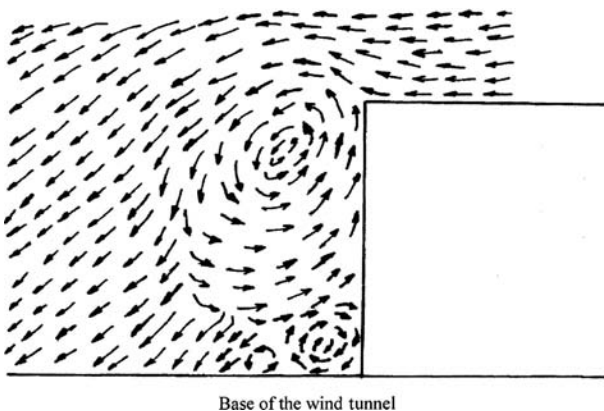


**Fig. 7** Flow pattern in the wake of the vehicle for zero r/min of the cylinder

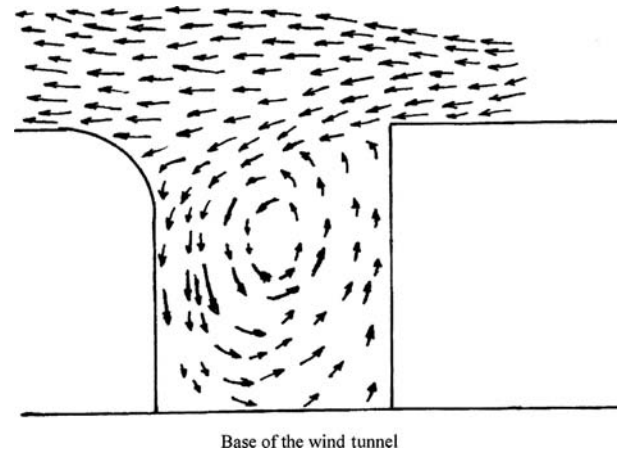


**Fig. 8** Wake region in the gap for 1 cm cylinder rotating at 2000 r/min

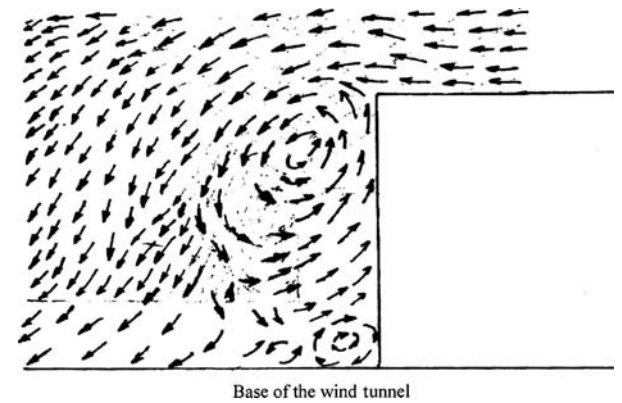


**Fig. 9** Flow pattern in the wake region for 1 cm cylinder rotating at 2000 r/min

The same experimentation was carried out at higher rotating speeds of the cylinder. Figures 10 and 11 similarly show the effect at a higher speed of 4000 r/min ( $\lambda = 0.16$ ) and it is seen that effect is more pronounced at higher speed, resulting in greater

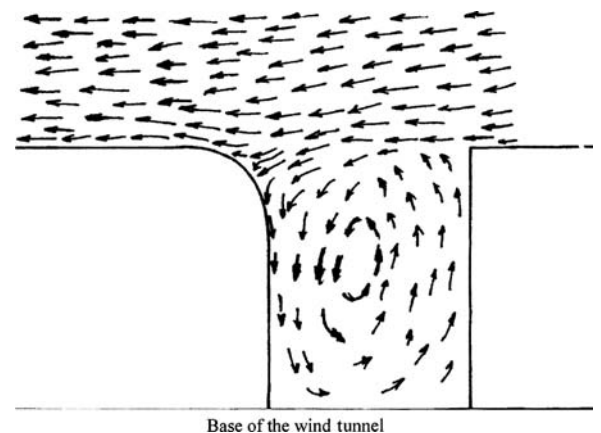


**Fig. 10** Wake region in the gap for 1 cm cylinder rotating at 4000 r/min

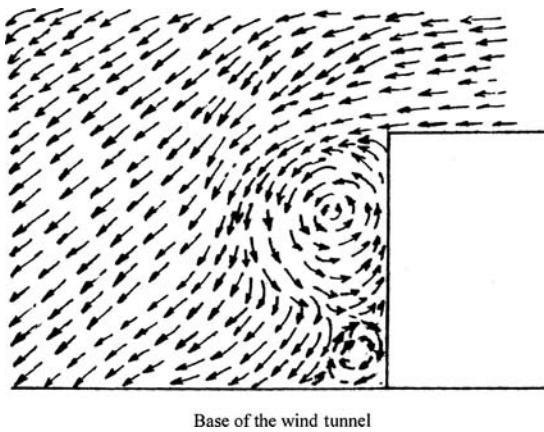


**Fig. 11** Flow pattern in the wake region for 1 cm cylinder rotating at 4000 r/min

injection and greater reduction in the wake region. As expected here, the drag coefficient reduced by 35 per cent to 0.32.

Similar analysis was carried out for a 2 cm radius rotating cylinder. Figures 12 and 13 show the wake and suction region respectively for a simulation with 2 cm radius and 2000 r/min ( $\lambda = 0.16$ ). This simulation resulted in very effective reduction even at low r/min as compared to the previous case. The drag coefficient came down to 0.38, a reduction of 25 per cent. The wake and suction region for a speed of 4000 r/min ( $\lambda = 0.32$ ) are shown in Figs 14 and 15 respectively. As a result of increase in r/min, the drag coefficient further reduces to 0.33.

Simulations for both the cylinder sizes were also done at a higher r/min of 5000 ( $\lambda = 0.20$  and  $\lambda = 0.40$ ) and it was observed that the drag force increased. Close observation of the flow pattern showed that the wake size increased for higher r/min due to rebounding of flow from the truck surface downstream of the rotating cylinders.

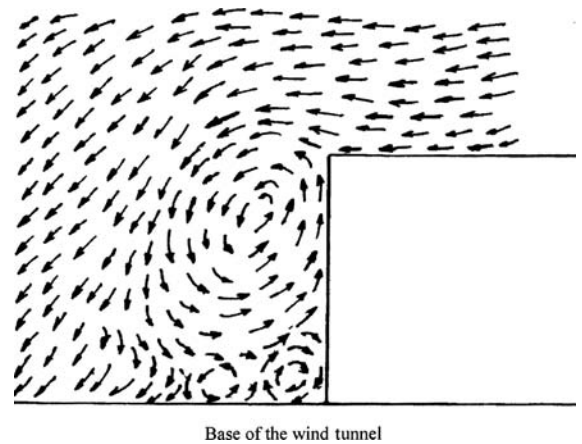


**Fig. 13** Flow pattern in the wake region for 2 cm cylinder rotating at 2000 r/min

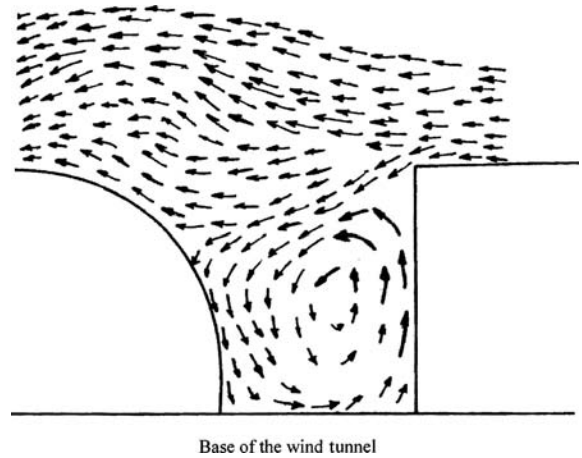


**Fig. 14** Wake region in the gap for 2 cm cylinder rotating at 4000 r/min

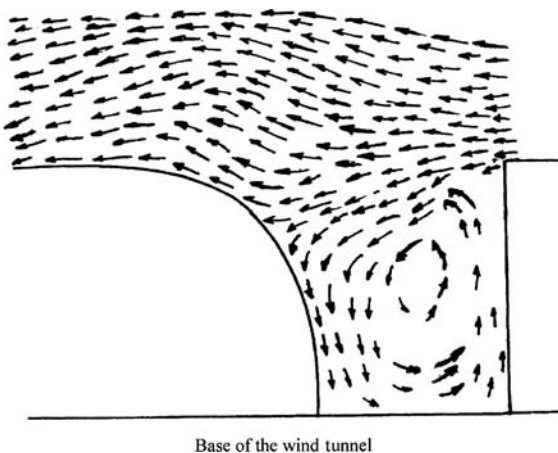


**Fig. 12** Wake region in the gap for 2 cm cylinder rotating at 2000 r/min

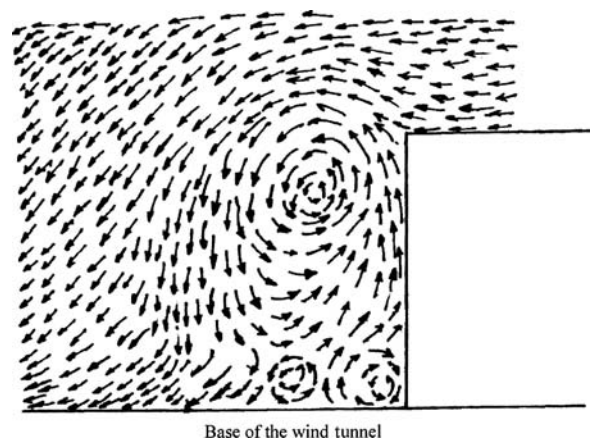


**Fig. 15** Flow pattern in the wake region for 2 cm cylinder rotating at 4000 r/min

## 4 CONCLUSIONS

Comparison of the experimental results with the FLUENT® results show that the realizable k- $\epsilon$  model is the most suitable turbulence model for modelling the airflow around a truck. Application of a rotating cylinder helped in attachment of the flow to the wall and hence delaying the separation of the boundary layer. Consequently, the aerodynamic drag was significantly reduced by 35 per cent. It was observed that the reduction in aerodynamic drag was the same for a 1 cm radius with 4000 r/min ( $\lambda = 0.16$ ) and a 2 cm radius with 2000 r/min ( $\lambda = 0.16$ ), implying that it is the overall linear velocity that finally results in the injection of momentum and reduction in drag. Also, the effect of momentum injection is pronounced in a certain range only and the r/min cannot be increased limitlessly. Overall this investigation highlights the importance of using rotating cylinders to induce momentum injection, thereby reducing the aerodynamic drag of the vehicle and provides a sound base for future work in this relatively unexplored area.

## ACKNOWLEDGEMENTS

The model was fabricated in the departmental workshop. The assistance of Mr Sita Ram, Senior Technician, in the design and construction of the model is gratefully acknowledged.

## REFERENCES

- 1 **Hucho, W. H.** *Aerodynamics of Road Vehicles*, 1997 (Cambridge University Press, Cambridge, UK).
- 2 **Lachmann, G. V.** *Boundary Layer and Flow Control*, Vols I and II, 1996 (Pergamon Press, Oxford, UK).
- 3 **Goldstein, S.** *Modern Developments in Fluid Mechanics*, Vols I and II, 1968 (Oxford University Press, Oxford, UK).
- 4 **Chang, P. K.** *Separation of Flow*, 1970 (Pergamon Press, Oxford, UK).
- 5 **Schlichting, H.** *Boundary Layer Theory*, 1968 (McGraw Hill Book Company, Maidenhead, UK).
- 6 **Rosenhead, L.** *Laminar Boundary Layers*, 1966 (Oxford University Press, Oxford, UK).
- 7 **Lissaman, P. B. S.** and **Lambie, J. H.** Reduction of aerodynamic drag of large highway truck. Proceedings of the conference/workshop on *The Reduction of the Aerodynamic Drag of Trucks*, California Institute of Technology, 10–11 October 1974, pp. 89–120 (National Science Foundation RANN Document Centre, Washington DC).

- 8 **Kirsh, J. W.** and **Bettes, W. H.** Feasibility study of the S<sup>3</sup> air vane and other truck drag reduction devices. Proceedings of the conference/workshop on *The Reduction of the Aerodynamic Drag of Trucks*, California Institute of Technology, 10–11 October 1974, pp. 89–120 (National Science Foundation RANN Document Centre, Washington DC).
- 9 **Montoys, L. C.** and **Streers, L. L.** Aerodynamic drag reduction tests on a full scale tractor-trailer combination with several add on devices. Proceedings of the conference/workshop on *The Reduction of the Aerodynamic Drag of Trucks*, California Institute of Technology, 10–11 October 1974, pp. 65–88 (National Science Foundation RANN Document Centre, Washington DC).
- 10 **Singh, S. N., Veeravalli, S. V., Bhatnagar, A., and Puri, P.** Effect of boundary layer control using momentum injection on the lift characteristics of a NACA airfoil. Proceedings of the 2nd International conference and 29th national conference of *Fluid Mechanics and Fluid Power*, IIT Roorkee, India, 13–15 December 2002, Vol. I, pp. 252–259 (Ajay Printers and Publishers, Roorkee).
- 11 **Modi, V. J., Mokhtarian, F., and Yokomizo, T.** Effect of moving surfaces on the airfoil boundary layer control. *J. Airc.*, 1990, **27**(1), 42–50.
- 12 **Modi, V. J., Mokhtarian, F., and Yokomizo, T.** Bound vortex boundary layer control with application to V/STOL airplanes. *Fluid Dyn. Res.*, 1 September 1988, **3**(1–4), 225–230.
- 13 **Hoerner, S. F.** *Fluid Dynamic Drag*, 1965 (US Library of Congress catalog card no. 64-19666).
- 14 **Fluent Inc.** *FLUENT 6.0 User's Guide*, NH03766, Vols 1–4, 2002 (Fluent Incorporated, Lebanon).
- 15 **Patankar, S. V.** *Numerical Heat Transfer and Fluid Flow*, 1978 (Hemisphere Publishing Corporation, New York, USA).

## APPENDIX

### Notation

$F$	body force per unit volume
$g$	gravitational acceleration
$p$	pressure
$u$	velocity
$\delta$	Kronecker delta
$\lambda$	speed ratio = surface velocity on the cylinder surface/free stream velocity
$\mu$	dynamic viscosity
$\rho$	density of fluid
$\tau$	shear stress

### Suffix

i, j, l tensorial notations